Cell and protein-compatible bioprinting of mechanically strong constructs for bone repair

MJ Sawkins[1,3], P Mistry[1], BN Brown[2,4], KM Shakesheff[1], LJ Bonassar[2] and J Yang[1]

[1]Tissue Engineering Group, School of Pharmacy, University of Nottingham NG7 2RD, UK

[2]Department of Biomedical Engineering, Sibley School of Mechanical and Aerospace Engineering, Cornell University, Ithaca, NY, USA

[3]Current address: Tissue Engineering Research Group, Department of Anatomy, Royal College of Surgeons in Ireland, 123 St. Stephen's Green, Dublin 2, Ireland; Trinity Centre for Bioengineering, Trinity College Dublin, Dublin 2, Ireland; Advanced Materials and Bioengineering Research (AMBER) Centre, RCSI & TCD

[4]Current address: McGowan Institute for Regenerative Medicine, Department of Bioengineering, University of Pittsburgh, Pittsburgh, PA, USA.

Abstract

Rapid prototyping of bone tissue engineering constructs often utilizes elevated temperatures, organic solvents and/or UV light for materials processing. These harsh conditions may prevent the incorporation of cells and therapeutic proteins in the fabrication processes. Here we developed a method for using bioprinting to produce constructs from a thermoresponsive microparticulate material based on poly(lactic-co-glycolic acid) at ambient conditions. These constructs could be engineered with yield stresses of up to 1.22 MPa and Young's moduli of up to 57.3 MPa which are within the range of properties of human cancellous bone. Further study showed that protein-releasing microspheres could be incorporated into the bioprinted constructs. The release of the model protein lysozyme from bioprinted constructs was sustainted for a period of 15 days and a high degree of protein activity could be measured up to day 9. This work suggests that bioprinting is a viable route to the production of mechanically strong constructs for bone repair under mild conditions which allow the inclusion of viable cells and active proteins.

1. Introduction

Recent years have seen the development of a number of approaches utilising additive manufacturing techniques such as selective laser sintering [1, 2], stereolithography [3-5], fused filament fabrication [6-8] and 3D printing [9-12] for the production of custom, defect-matched constructs for bone repair. These approaches require the ceramic and polymeric materials which are used with them to be processed by the application of high temperatures [2, 6-8, 10, 11], ultraviolet light [3-5] or organic solvents [9, 12]. Whilst these harsh processing conditions cause little concern for the production of acellular scaffolds they have prevented the incorporation of cells and therapeutic biomolecules during the fabrication process. Post-fabrication addition of proteins and cells is often associated with the inability to provide long-term delivery and uneven seeding respectively. More importantly, it prevents these elements from being patterned within constructs to create functional heterogeneity. It is therefore important to develop production processes which are compatible with the inclusion of cells and biomolecules.

Bioprinting may provide a solution to this problem since it allows the fabrication of tissue engineered constructs at ambient conditions. To-date this approach has predominantly been used to produce hydrogel constructs since these are typically the only class of materials which can be processed under such mild conditions [13-20]. However there are issues with the use of hydrogel materials in orthopaedic applications including the very large disparity between their mechanical properties and those of bone [14, 15, 19, 20]. In

addition to the inability of such weak materials to endure relevant *in vivo* loads, the low stiffness of hydrogels may inhibit the osteogenic differentiation of both endogenous and exogenous stem cells [21].

A thermoresponsive microparticulate material based on a blend of poly(L-lactic-co-glycolic acid) (PLGA) and polyethylene glycol (PEG) may overcome these issues. When mixed with aqueous carrier fluids at room temperature, these PLGA-based microparticles form extrudable pastes which can be formed to the desired scaffold shape. Incubation of these pastes at 37˚C and surrounded by aqueous fluid leads to thermoresponsive liquid sintering and the formation of porous solid constructs [22-27]. These constructs can be engineered with mechanical properties which are comparable to those of human cancellous bone [22-25, 28-31]. Previous studies utilising this material have shown that proteins [24, 26, 27] and cells [22, 24] can tolerate the mixing and extrusion processes whilst maintaining activity and viability respectively. Encapsulated proteins can be delivered over several weeks [27] and the microporosity which is inherent to these constructs may also have beneficial effects on tissue ingrowth and angiogenesis *in vivo*.

The primary purpose in developing this material was to formulate an injectable bone defect filler but we postulated that its ability to be delivered by injection would also make it highly suitable for use with extrusion based additive manufacturing techniques. Presented here is the first assessment of the feasibility of using the Fab@Home bioprinting platform [14, 17, 18, 32] in conjunction with PLGA-based microparticle pastes to fabricate bone tissue engineering constructs at ambient conditions. Particular emphasis is placed on achieving the incorporation of viable cells and active proteins into the bioprinting process to produce living constructs which have appropriate mechanical properties for implantation into bone defects.

2. Materials & Methods

2.1. Production and Sintering of PLGA/PEG Blend Microparticles

Poly(lactic-co-glycolic acid) (PLGA) (85:15 lactide:glycolide, 53 kDa, Evonik Biomaterials, Birmingham, AL, USA) was melt blended at 90^{o}C with poly(ethylene glycol) (PEG) (400 Da, Clariant, Leeds, UK) in a 93.5:6.5 (w:w) ratio. This melt blend was then milled in a Krups F203 mill which had been pre-cooled with liquid nitrogen. The resulting powder was manually sieved using analytical test sieves (Retsch (UK), Castleford, UK) to select the 50 – 100 μm size fraction.

To produce constructs these PLGA-PEG microparticles were suspended in aqueous carrier fluids to form dense pastes which were dispensed via bioprinting and then sintered by incubation in a humidified environment at 37^{o}C for two hours, followed by submersion in 0.9% (w/v) sodium chloride in the same environment for a further 22 hours.

2.2. PLGA-Based Microsphere Manufacture

PLGA-PEG-PLGA triblock copolymer ('Triblock') was fabricated by a previously-published protocol [33]. Gel permeation chromatography measurements of the synthesized triblock copolymer using a PL-GPC 120 (Polymer Labs) indicated a molecular weight of 4590 Da and a polydispersity index of 1.60.

PLGA and Triblock were dissolved in dichloromethane at 14 and 6% (w/v) respectively to a total polymer mass of 1 g. A small amount of water (2% (v/v) relative to the organic phase) was added to the polymer solution and this combination was homogenized for two minutes to form a primary emulsion using a Silverson L5M homogenizer (Silverson Machines Ltd., Chesham, UK) at 4000 rpm. The primary emulsion was then added to an aqueous solution of 0.3% (w/v) poly(vinyl alcohol) (PVA, 87 – 89% hydrolysed, 13 – 23 kDa, Sigma-Aldrich) and homogenized for two minutes at 2000 rpm to form a secondary emulsion. The secondary emulsion was stirred for 4 hours and the hardened microspheres collected under vacuum

filtration (0.2 µm filter mesh), snap frozen in liquid nitrogen and lyophilized for 48 hours. Lysozyme was incorporated into microspheres by dissolution in the water used to form the primary emulsion (9 mg human serum albumin carrier protein (Sigma-Aldrich) and 1 mg lysozyme from chicken egg white (Sigma-Aldrich)). Primary emulsion production was carried out in 30 mL PTFE beakers (VWR International, Lutterworth, UK) and secondary emulsion in a 250 mL borosilicate glass beaker (Fisher Scientific) using 200 mL of PVA solution.

2.3. Immortalized Human Mesenchymal Stem Cells

Primary hMSCs (bone marrow-derived, TCS Cellworks, Buckingham, UK) were immortalized (ihMSCs) using a previously published protocol [34]. ihMSCs were cultured in Dulbecco's modified Eagle medium (Life Technologies, Paisley, UK) supplemented with 10% (v/v) foetal bovine serum (Sigma-Aldrich, Poole, UK), 1% (v/v) L-glutamine (Sigma-Aldrich), 1% (v/v) penicillin /streptomycin (Life Technologies) and 1% (v/v) non-essential amino acids (Sigma-Aldrich). Cultures were maintained at 37^{o}C and 5% (v/v) CO_2 as monolayers on tissue culture treated polystyrene. At 80% confluency cells were passaged by trypsinisation and reseeded between 1/5th and 1/8th of pre-passage density.

2.4. Bioprinting of PLGA-PEG Microparticle Pastes

The Fab@Home platform (Model 2) [35] was used in conjunction with 16G tapered dispense tips (Adhesive Dispensing, Milton Keynes, UK) for microparticulate construct fabrication. To prevent early sintering of microparticles all materials were pre-cooled to 4^{o}C and wherever possible sample preparation was carried out at this temperature as well. PLGA-PEG microparticles with or without a proportion of PLGA-based microspheres were mixed with aqueous carrier solutions containing one of the following viscosity modifiers - medium viscosity carboxymethyl cellulose (CMC) (catalogue number 12M8P, Ashland Speciality Ingredients, Poole, UK), high viscosity CMC (catalogue number 12M31P, Ashland) or Pluronic® F-127 (Sigma-Aldrich). The concentrations of these modifiers were in the range 0.1 – 4% (w/v) and the solutions were mixed with the solid components at various v:w ratios in the range 1:1 – 1.7:1. The resulting pastes were loaded into syringe barrels for deposition using a material flow rate of 38.8 µL s^{-1}.

For the accuracy of unconfined compression testing it was important that bioprinted constructs had identical shapes and sizes and that they could be tested without the need for them to be trimmed. In order to achieve this PLGA-based microparticulate pastes were extruded into poly(tetrafluoroethylene) (PTFE) cylindrical moulds 6 mm in diameter and 12 mm in height. The current printing resolution is insufficient for producing such compression testing samples with precise shape and uniformity.

In order to incorporate cells into bioprinted pastes, suspensions of ihMSCs in PBS were first manually mixed by stirring with acellular solutions of high viscosity CMC to a final CMC concentration of 2% (w/v) and a final cell density of 2 x 10^{6} mL^{-1}. The resulting cell suspensions were then combined with microparticles in a 1.4:1 (v:w) ratio for bioprinting.

2.5. Unconfined Compression Testing

Three sintered constructs per condition were subjected to unconfined compression testing using a TA.HDplus texture analyser (Stable Micro Systems, Godalming, UK). Samples were tested at 37^{o}C immediately at the end of 24 hours sintering. The probe movement rate was 0.04 mm s^{-1} (which equates to a 0.333% s^{-1} strain rate) and the test was continued to 50% strain.

2.6. Scanning Electron Microscopy and Micro-Computed Tomography

SEM was performed using a JSM 6060LV (JEOL, Welwyn Garden City, UK). Images were taken at a minimum of three different magnifications and in three different quadrants of each sample and three samples were imaged per condition. Micro-computed tomography (µCT) imaging was undertaken using a Skyscan 1174 (Bruker microCT, Kontich, Belgium). This analysis was performed on three samples per condition. Images were taken at 6.7 µm resolution every 0.4^{o} of rotation from 0 to 180^{o} and at each rotation step a total of 6 frames were averaged to produce the final image. The NRecon software provided by the manufacturer was used to reconstruct cross-sectional slices with ring artefact reduction set to 20, beam hardening to 20% and consistent thresholding across all samples. Finally CTAn was used to produce three-dimensional models of scanned samples and to perform analyses such as measurements of total porosity and pore size distribution. As with reconstruction in NRecon, consistent thresholding was applied across all samples to be compared and despeckling was also performed to remove objects of 100 voxels or less from reconstructed images prior to analysis and modelling.

2.7. Measurement of Protein Release Rate from Microspheres

To produce constructs for assessment of post-bioprinting lysozyme release rate and activity microparticle/microsphere mixtures were formulated into pastes using 2% (w/v) high viscosity CMC at a 1.4:1 (v:w) ratio. Pastes containing 400 mg of solid were then extruded into PTFE moulds and sintered for two hours prior to submersion in 3 mL of pre-warmed (37^{o}C) PBS in 15 mL centrifuge tubes to initiate protein release. This study was conducted in triplicate and compared constructs containing lysozyme-loaded microspheres with those containing blank microspheres. Incubation was continued at 37^{o}C for a period of 15 days under gentle agitation and at regular intervals the PBS was completely aspirated, assayed for total protein content and lysozyme activity and replaced.

The Micro BCA Protein Assay Kit (Fisher Scientific) was used to quantify the total protein content of aspirated release medium. As per manufacturer's instructions 150 µL of each sample or standard was mixed in a 96-well plate well in triplicate with 150 µL of complete working reagent. After 2 hours incubation at 37^{o}C, the absorbance of the mixture in each well was measured at 562 nm.

The ability of lysozyme to lyse *Micrococcus lysodeikticus* bacteria was used to measure protein activity in release medium, which was compared to the total lysozyme released as calculated from BCA assay results. In triplicate in the wells of a 96-well plate 150 µL of each standard or sample was mixed with 100 µL of 2.3 mg mL^{-1} *M. lysodeikticus* suspension (Sigma-Aldrich). The drop in absorbance due to cell lysis over a three minute period was then read at 450 nm at 37^{o}C.

2.8. Viability Assessment of Cells in PLGA-PEG Pastes

Pre-bioprinting ihMSC counting and viability assessment were performed using an improved Neubauer haemocytometer and trypan blue (Fisher Scientific, Loughborough, UK) dye exclusion. The extruded material was incubated at 37˚C in humidified environment for 30mins to allow the particles to fuse before immersion in culture medium. For each time point, three samples were made. For imaging cells, the extruded constructs were disassembled manually to expose the cells and then submerged in a 2µM/4µM calcein AM/ethidium homodimer-1 (live/dead) solution (Life Technologies) and incubated for 45 minutes. Samples were imaged using a Leica DM IRB inverted microscope (Leica Microsystems (UK), Milton Keynes, UK). Six fields of view were imaged for each of three samples to assess cell viability.

2.9. Statistical Analysis

The homogeneity of variances across experimental groups was determined by Levene's test. Appropriate *post hoc* procedures were used after one way ANOVA for pairwise comparison of experimental groups. In cases of equal variance Tukey's procedure was applied, whilst the Games-Howell procedure was used for cases of unequal variance. All statistical tests were performed at the 5% significance level. For comparing cell viability, two-way ANOVA and Tukey's test were used with a α level of 0.05.

3. Results & Discussion

3.1. Feasibility of Bioprinting PLGA-Based Microparticulate Pastes

The PLGA-based microparticulates used in this work must be suspended in the carrier liquid at high densities to generate large numbers of bridging contacts and consequently sufficient mechanical strength. Meanwhile, the mixture of microparticulates and liquid carrier needs to be extruded with consistent composition using the Fab@home model 2 bioprinting platform. We demonstrated that it was feasible to deposit the mixture using bioprinting by selecting the appropriate microparticle size, solid to carrier ratio and carrier concentration. Extruded microparticulate material could be sintered in PBS by a thermoresponsive sintering mechanism in which the glass transition temperature rose due to the leaching of the PEG compoonent. The size and shape of the bioprinted constructs were maintained after sintering, and sufficient mechanical integrity was acquired to allow handling and manipulation (figure 1).

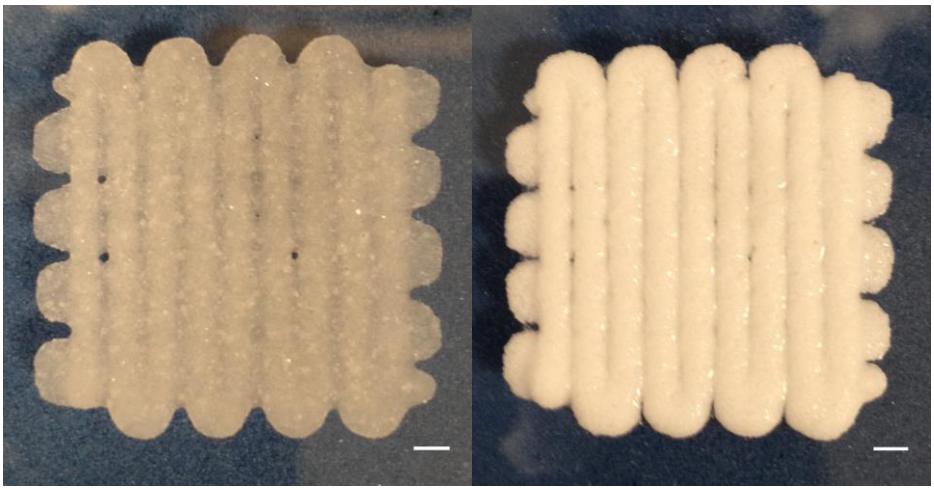

Figure 1 – Representative images of constructs produced via bioprinting of PLGA-PEG microparticles suspended in 3% medium viscosity CMC at a 1.4:1 (v:w) ratio of aqueous carrier to solid. Images are shown of constructs both before (left) and after (right) 24 hours sintering. Scale bars represent 2 mm.

In order to allow consistent and controlled extrusion, the microparticulate pastes used in this study differed in several ways from those used in previous studies [22-27]. To prevent syringe tips from becoming clogged smaller microparticles were used than in previous studies, with the 50 – 100 µm size fraction isolated in place of the 100 – 200 µm fraction. In addition, to prevent syneresis (preferential ejection of the fluid component), a greater proportion of carrier fluid was used (carrier to solid ratio of 1.4:1 as opposed to 0.6:1 – 1:1) and the concentration of medium viscosity CMC in the fluid was also increased (3% (w/v) as opposed to 0.5% (w/v)). Avoiding clogging and achieving 'complete extrusion' of the entire paste volume was considered a pre-requisite for ensuring that paste composition and thus ultimate mechanical properties remained consistent throughout fabrication.

3.2. Optimising the Mechanical Properties of Bioprinted Constructs

The next stage in the development of this bioprinting-based approach to fabricate constructs was to optimize the process with respect to mechanical properties. To achieve this aim, alternative viscosity modifiers were considered alongside the medium viscosity CMC used up to this point. The minimum carrier to solid (v:w) ratios that permitted complete extrusion of microparticle pastes without syringe tip clogging are shown in Table 1. Pluronic® F127 was investigated alongside CMC as having potential to directly lubricate microparticle-microparticle interactions. It was found that as well as requiring larger ratios than the best concentrations of CMC to achieve complete extrusion (table 1), all concentrations of Pluronic® F127 produced pastes which displayed liquid-like behaviour after deposition and did not allow structures or patterns to be maintained through the sintering process.

It can be reasonably expected that a larger proportion of carrier leads to less microparticle-to-microparticle contacts and thus lower mechanical strength. The conditions which allowed the least liquid carrier to be used to achieve consistent extrusion without the syringe tips becoming clogged were considered optimal and were carried forward for further evaluation. On the basis of the results shown in table 1 the three most promising carriers were 3% (w/v) medium viscosity CMC, 2% (w/v) high viscosity CMC and 3% (w/v) high viscosity CMC.

Table 1 – Minimum v:w ratios of a variety of aqueous carriers to solid required to produce PLGA-PEG microparticle pastes which could be extruded in their entirety by Fab@Home Model 2 bioprinting platform. Failure to achieve 'complete extrusion' indicates syneresis, tip clogging and inconsistent paste composition.

Carrier	Minimum Carrier to Solid Ratio (v:w)
0.5% (w/v) Medium Viscosity CMC	1.7:1
1% (w/v) Medium Viscosity CMC	1.7:1
2% (w/v) Medium Viscosity CMC	1.6:1
3% (w/v) Medium Viscosity CMC	1.4:1
0.5% (w/v) High Viscosity CMC	1.7:1
1% (w/v) High Viscosity CMC	1.5:1
2% (w/v) High Viscosity CMC	1.4:1
3% (w/v) High Viscosity CMC	1.3:1
0.5% (w/v) Pluronic® F127	1.6:1
1% (w/v) Pluronic® F127	1.5:1
2% (w/v) Pluronic® F127	1.5:1
3% (w/v) Pluronic® F127	1.5:1

The mechanical properties of constructs produced using the chosen combinations were then assessed using unconfined compression testing, both at the derived minimum ratios of carrier to solid and at ratios either side. Close rations at either side of the minimum ratios were selected because tip clogging was sensitive to small changes in the carrier/solid ratio. The additional ratios were intended to indicate in principle whether any additional mechanical strength could be obtained by intentionally making the pastes 'too wet' or 'too dry'. On the basis of the yield stresses (figure 2) and Young's moduli (figure 3) of bioprinted constructs, 2 and 3% (w/v) high viscosity CMC (both at minimum ratios) appeared to be the most promising carriers for construct fabrication. These constructs had yield stresses of 1.22 and 1.15 MPa and Young's moduli of 54.4 and 57.3 MPa respectively. These values are lower than those obtained in other bone tissue engineering studies

with harsher fabrication processes [1-4, 8, 10-12] but are nonetheless within the normal ranges for cancellous bone [28-31, 36, 37].

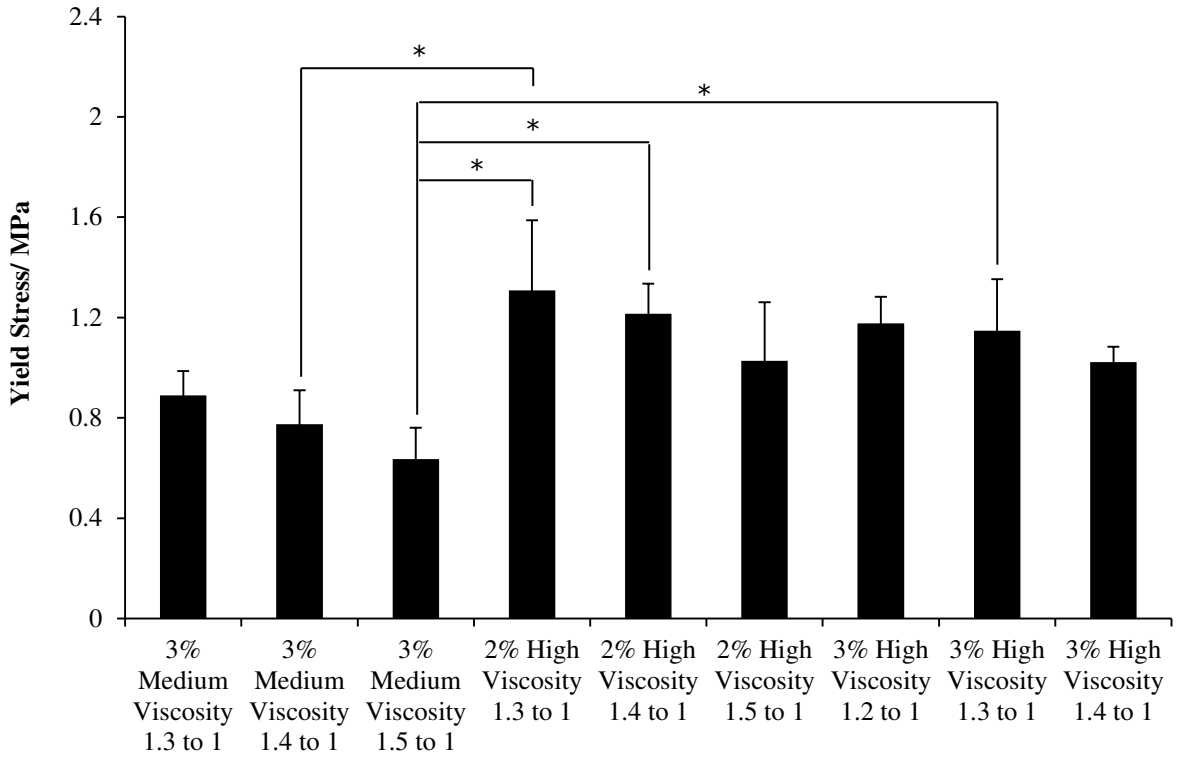

Figure 2 – Yield stresses for bioprinted PLGA-PEG microparticulate scaffolds as assessed by unconfined compression testing (n = 3). PLGA-PEG microparticles were suspended in a variety of aqueous carriers at a variety of carrier to solid (v:w) ratios for bioprinting into cylindrical PTFE moulds. Samples were tested after 24 hours sintering. Error bars show one standard deviation and statistically-significant differences are denoted by (*).

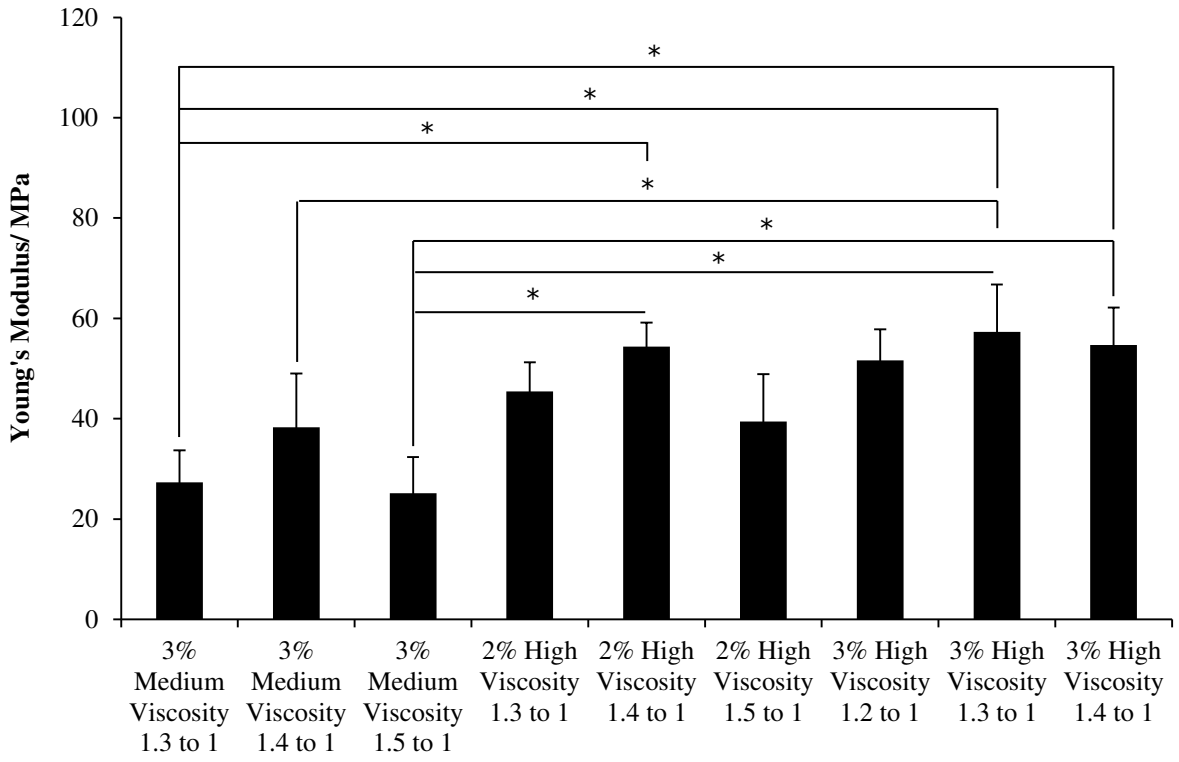

Figure 3 – Young's moduli for bioprinted PLGA-PEG microparticulate scaffolds as assessed by unconfined compression testing (n = 3). PLGA-PEG microparticles were suspended in a variety of aqueous carriers at a variety of carrier to solid (v:w) ratios for bioprinting into cylindrical PTFE moulds. Samples were tested after 24 hours sintering. Error bars show one standard deviation and statistically-significant differences are denoted by (*).

In general, constructs dispensed with high viscosity carriers showed higher mechanical properties than those produced with the medium viscosity carrier. In a construct produced using medium viscosity CMC there is likely to be a more heterogeneous distribution of microparticles, creating 'strong points' and 'weak points' within the structure. The mechanical behaviour of the constructs will then result from the properties of the weak points more than the strong and the constructs as a whole will be less strong and yield more readily. This effect will be lessened in constructs produced using the high viscosity carriers as these are more effective at preventing syneresis and ensuring homogeneous distributions of microparticles.

Compression testing showed no significant differences between constructs produced using the same carrier with different carrier to solid ratios and so subsequent analysis was performed only on the central ratios. µCT and SEM imaging were used to measure and visualise the pore structures of constructs produced using the different carrier solutions. Constructs produced using 2 and 3% (w/v) high viscosity CMC had relatively low porosities of 10.8 and 12.4% respectively (figure 4) and these values are reflected in the relatively dense structures seen via SEM imaging (figure 5). Constructs produced using medium viscosity CMC as a carrier showed porosities which were not statistically different to those of other constructs. However the variability seen with this carrier was much higher than with others. This again suggested the inability of medium viscosity CMC to prevent syneresis, which resulted in large variations in porosity between different constructs.

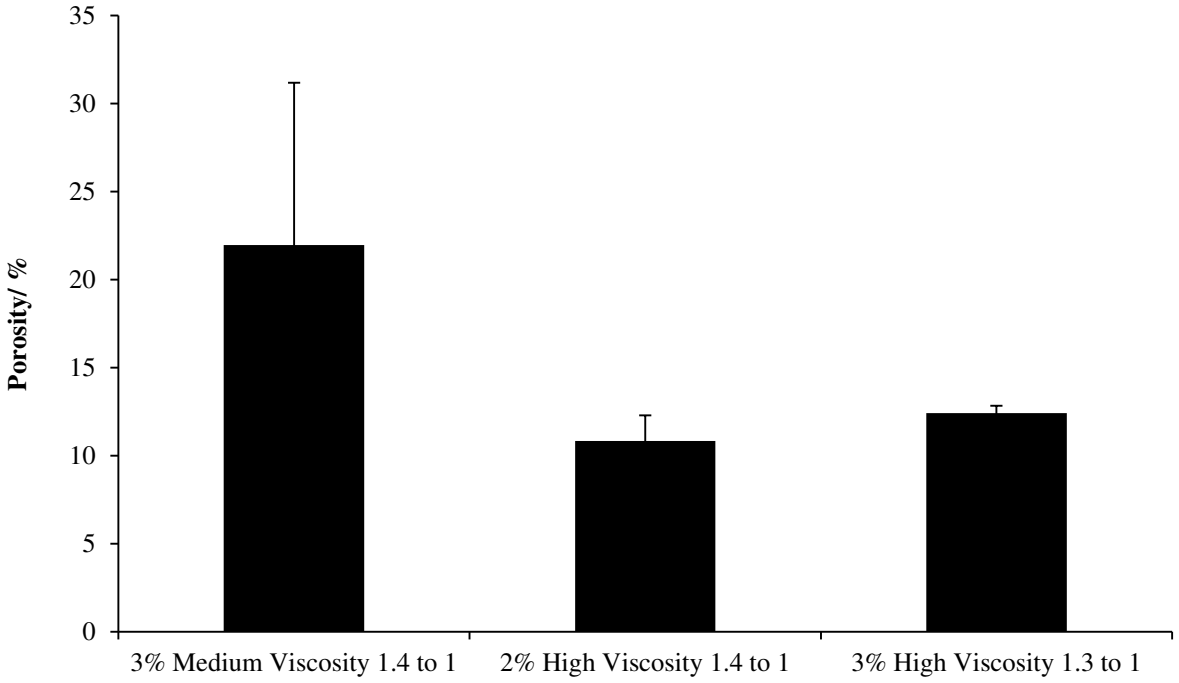

Figure 4 – Porosities of bioprinted PLGA-PEG microparticulate scaffolds as assessed by µCT imaging and analysis (n = 3). PLGA-PEG microparticles were suspended in a variety of aqueous carriers at different carrier to solid (v:w) ratios for bioprinting into cylindrical PTFE moulds. Samples were tested after 24 hours sintering. Error bars show one standard deviation.

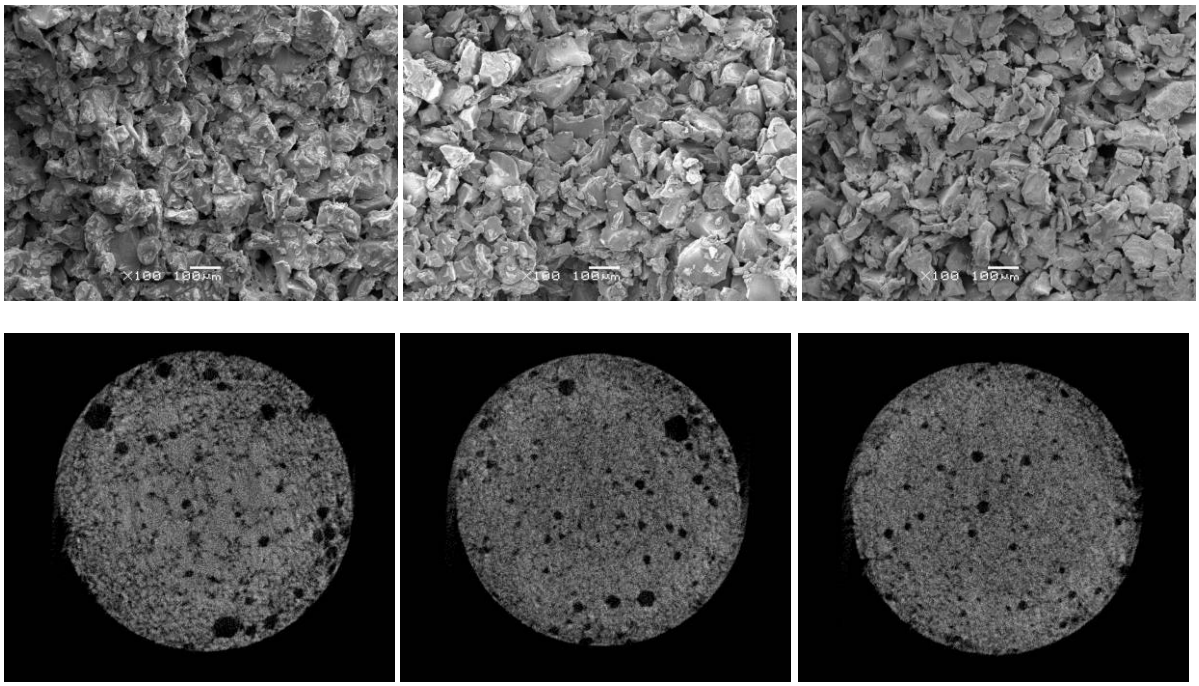

Figure 5 – SEM (upper row) and representative µCT (lower row) images of cross-sectional fracture surfaces of bioprinted PLGA-PEG microparticulate scaffolds. PLGA-PEG microparticles were suspended in a variety of aqueous carriers for bioprinting into cylindrical PTFE moulds. Constructs were fractured after 24 hours sintering. Left to right - 3% (w/v) medium viscosity CMC used at 1.4:1 (v:w) carrier to solid ratio, 2% (w/v) high viscosity CMC at 1.4:1 ratio and 3% (w/v) high viscosity CMC

at 1.3:1 ratio. All µCT images used for porosity and pore size measurement are shown in supplementary figure 1.

The mean pore sizes for constructs produced using 2 and 3% (w/v) high viscosity CMC carriers were 65.3 and 76.6 µm (figure 6). It was found that constructs produced using 2% (w/v) high viscosity CMC had statistically smaller mean pore sizes than those produced with other carriers. This may suggest that this carrier is the most effective at ensuring homogenous microparticle distribution. It has been suggested that an optimal construct for bone regeneration needs to contain a large population of pores of around 200 – 400 µm in size in order to maximize tissue ingrowth [38-41]. The pores produced here were mostly smaller than this suggested range but many were large enough to allow cell motion and proliferation in the constructs, based on the results of previous studies in bone tissue engineering [42, 43]. Additionally with appropriate development and optimisation it may be possible to create pores in this desired size range by designing them into the bioprinted construct architecture.

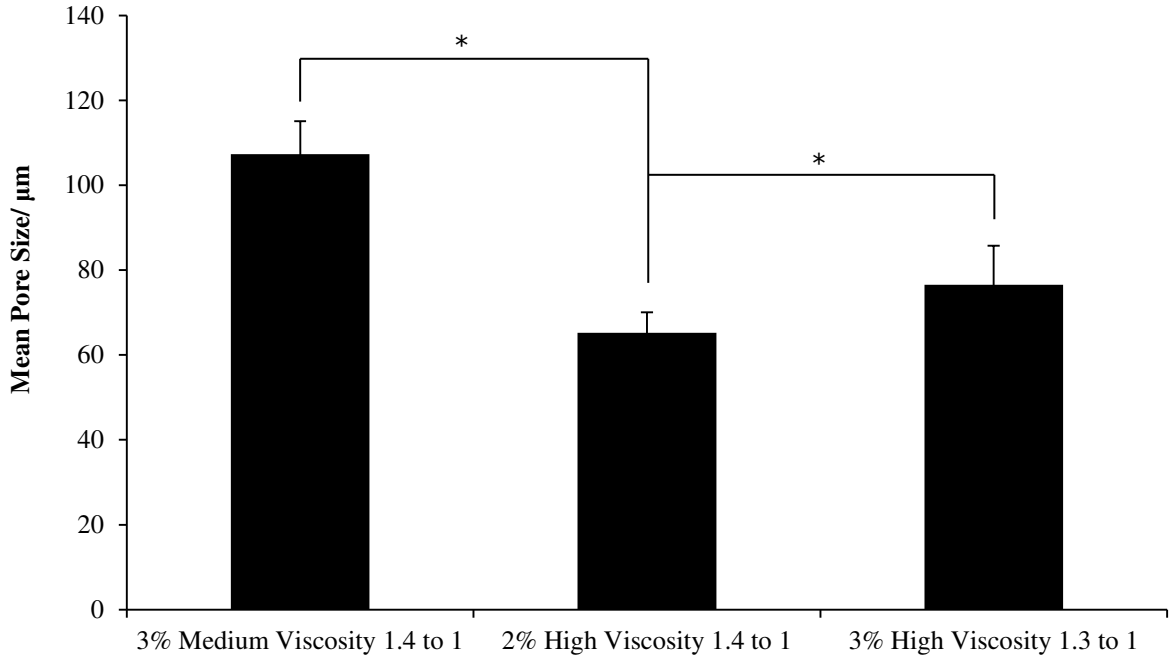

Figure 6 – Mean pore sizes of bioprinted PLGA-PEG microparticulate scaffolds as assessed by µCT imaging and analysis (n = 3). PLGA-PEG microparticles were suspended in a variety of aqueous carriers at different carrier to solid (v:w) ratios for bioprinting into cylindrical PTFE moulds. Samples were tested after 24 hours sintering. Error bars show one standard deviation and Statistically-significant ($p < 0.05$) differences are denoted by (*).

3.3. Incorporation of Cells and Proteins in Bioprinted Constructs

Besides achieving mechanical properties that match with bone, incorporating biological factors such as cells and growth factors in the scaffold can potentially accelerate healing of complex bone defects. The ability to print the PLGA-PEG material at ambient temperature enables the incorporation of temperature-sensitive components such as cells and proteins in a spatially defined manner. The differentiation of MSCs in moulded scaffolds made of PLGA-PEG and PLGA particles has been studied previously [44]. As an initial study, here we investigated the bioactivity and viability of

homogeneously incorporated proteins and cells. We first investigated the incorporation of therapeutic proteins. Using an approach utilized extensively by our group [33, 45] and others [5, 46-49] lysozyme was incorporated into PLGA-based microspheres by a water-in-oil-in-water double emulsion technique. A PLGA-PEG-PLGA triblock copolymer [33] was used to modify the protein release profile. Lysozyme was being used here as a model protein for bone morphogenetic protein-2, which is a potent growth factor involved in bone development and repair [50-53]. Lysozyme was chosen on the basis of the two proteins' similar molecular weights and isoelectric points. These protein-loaded microspheres were then incorporated into microparticle pastes used for bioprinting, with previous work suggesting a 3:1 (w:w) ratio of microparticles to microspheres as a suitable starting point [44].

A release study was undertaken to assess the controlled release of active protein from microspheres which had been incorporated into microparticulate pastes for bioprinting. In this study constructs containing lysozyme-loaded microspheres were found to be capable of delivering active protein for a period of at least 9 days (figure 7). The protein released by the microspheres was predominantly active (≥ 61%), with no clear drop in activity observed across this period. Beyond the ninth day after the start of the study the total activity of released protein dropped below the sensitivity of the *Micrococcus* assay, but protein release could be observed by micro BCA assay up to the fifteenth day (Supplementary Figure 2). This suggests that optimisation of the microsphere formulation would allow active protein to be delivered over significantly longer periods as in previous studies [45].

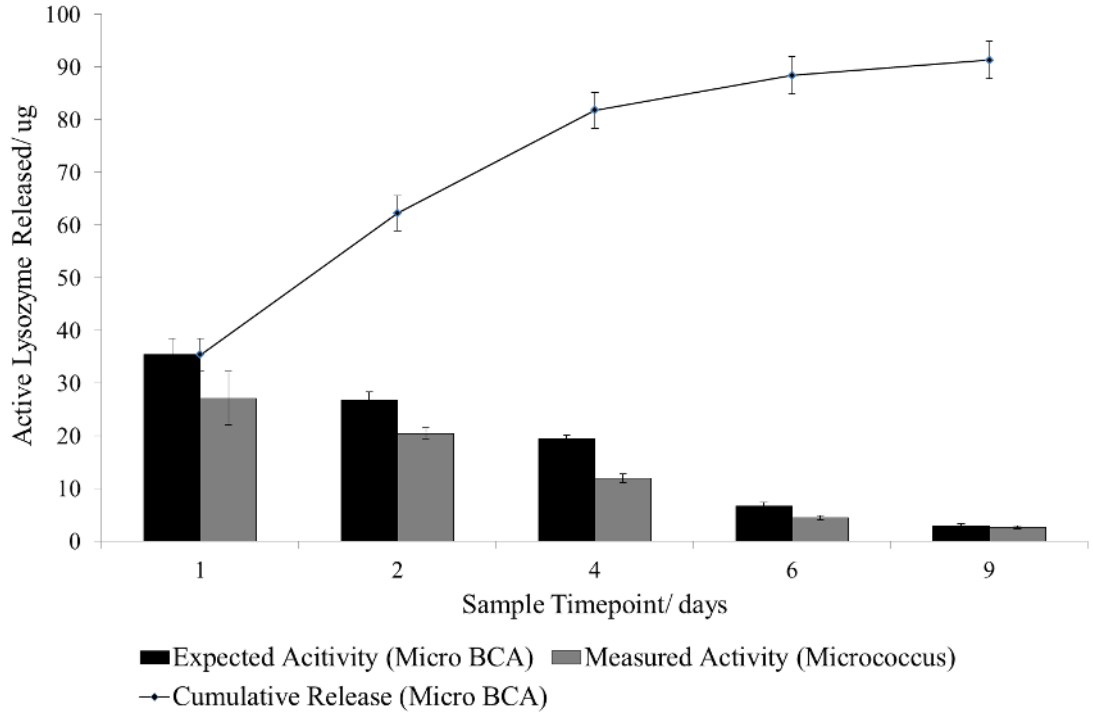

Figure 7 – Lysozyme release from PLGA microspheres encapsulated within bioprinted PLGA-PEG microparticulate constructs. A 9:1 (w:w) mixture of HSA and lysozyme was encapsulated in PLGA microspheres via a double emulsion protocol with a total protein content of 1% (w/w) relative to polymer. Expected activity levels are one tenth of total protein level measured by Micro BCA assay. Error bars represent one standard deviation.

The incorporation of non-sintering microspheres as described above can potentially lower the mechanical properties of PLGA-PEG microparticulate constructs by reducing the number of bridging contacts between the thermoresponsive microparticles. This effect needs to be addressed in future studies aimed at further optimising the construct production process. However, the reduction in mechanical strength may be lessened by reducing the proportion of microspheres in the constructs. Previous studies showed that the amount of protein encapsulated in a given mass of microspheres could be varied over approximately an order of magnitude whilst maintaining good encapsulation efficiency [33, 45, 54]. Increasing the ratio of protein to polymer would allow fewer microspheres to be incorporated whilst maintaining the total protein load per construct, and this would allow better retention of mechanical properties.

A further key step in the process development undertaken here was the incorporation of live cells in the production process. Cells were mixed manually using a plastic spatula into the microparticulate pastes and the effects of factors such as the cell density were not investigated at this stage. The viability of cells was found to be dependent on the carrier to solid ratio. The cell viabilities for the 1.5:1 ratio were 87% and 77% at day 0 and day 1, respectively. Decreased cell viabilities were found for a higher ratio (1.4:1) at both time points. The viability for the 1.4:1 ratio dropped below 50% at day 1. This demonstrated that a small change in carrier:particle ratio could have a significant effect on cell viability. The yield stress and Young's modulus for the 1.5:1 ratio material was lower than those of 1.4:1 but not statistically significant. We think that the significant drop in cell viability could be due to reduced lubrication resulted from a smaller amount of viscous carrier. A small reduction in lubrication could significantly increase the mechanical stress on cells during extrusion though a needle.

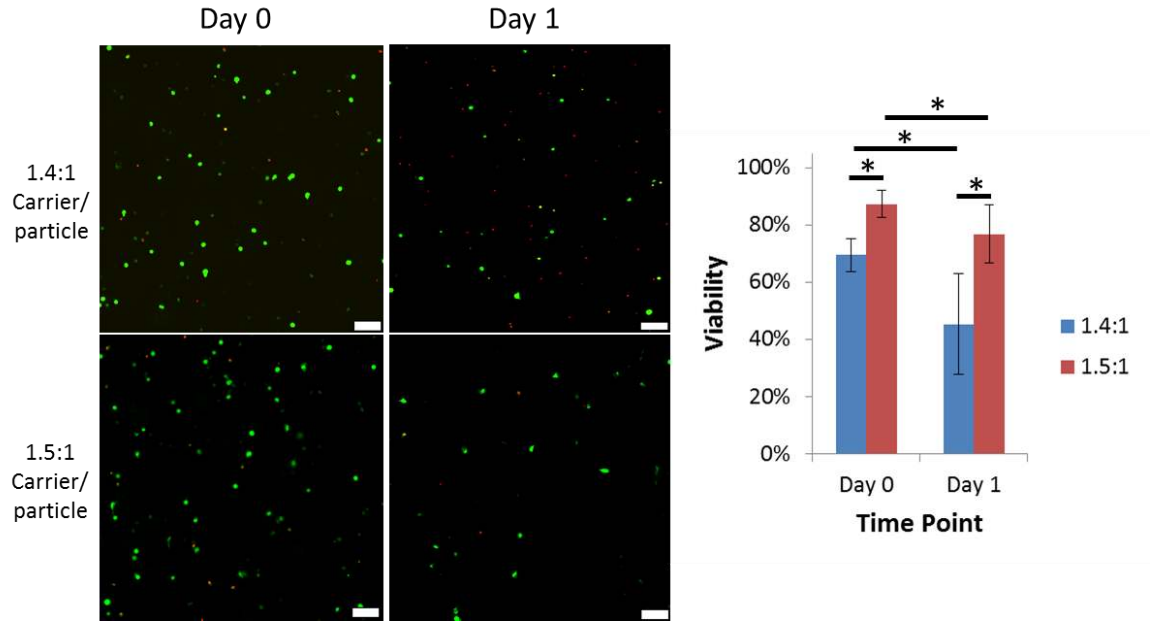

*Figure 8 – Fluorescence microscopy images of live/dead (calcein AM/ethidium homodimer-1) stained ihMSCs bioprinted at 2 million cells per mL in a microparticulate paste composed of PLGA-PEG microparticles suspended in 2% high viscosity CMC at two carrier to solid ratios (v:w).Data are presented as means±SD (n=18). * Data statistically analysed by two-way ANOVA and Tukey's test assuming confidence levels of 95% (p<0.05).Scale bar=100 µm*

4. Conclusions

The work presented here has demonstrated the essential feasibility of using bioprinting and a thermo-responsive material to produce constructs which have mechanical properties comparable to cancellous bone. The mild conditions used for bioprinting and material sintering have allowed viable cells and active therapeutic proteins to be incorporated into the construct production process. The approach adopted in this study has the potential for patterning biological constituents within constructs to achieve more sophisticated architectures, which circumvents the problems associated with post-fabrication cell seeding and biomolecule addition. The complexity of the final printed scaffold will depend on individual applications in which the scaffold is intended to be used.

Acknowledgments

The authors wish to thank and acknowledge Natasha Birkin (University of Nottingham) for conducting the GPC analysis of PLGA-PEG-PLGA triblock copolymer. The research leading to these results has received funding from the European Research Council under the European Community's Seventh Framework Programme (FP7/2007-2013)/ERC grant agreement 227845. The work on materials development was co-funded by the EPSRC Centre for Innovative Manufacturing in Regenerative Medicine.

References

1. Wiria, F.E., et al., *Poly-epsilon-caprolactone/hydroxyapatite for tissue engineering scaffold fabrication via selective laser sintering.* Acta Biomaterialia, 2007. **3**(1): p. 1-12.
2. Williams, J.M., et al., *Bone tissue engineering using polycaprolactone scaffolds fabricated via selective laser sintering.* Biomaterials, 2005. **26**(23): p. 4817-4827.
3. Melchels, F.P.W., et al., *Mathematically defined tissue engineering scaffold architectures prepared by stereolithography.* Biomaterials, 2010. **31**(27): p. 6909-6916.
4. Brandi, F., et al., *Rigid biodegradable photopolymer structures of high resolution using deep-UV laser photocuring.* Journal of Micromechanics and Microengineering, 2011. **21**(5): p. doi: 10.1088/0960-1317/21/5/054007.
5. Lee, J.W., et al., *Bone regeneration using a microstereolithography-produced customized poly(propylene fumarate)/diethyl fumarate photopolymer 3D scaffold incorporating BMP-2 loaded PLGA microspheres.* Biomaterials, 2011. **32**: p. 744-52.
6. Seyednejad, H., et al., *Preparation and characterization of a three-dimensional printed scaffold based on a functionalized polyester for bone tissue engineering applications.* Acta Biomaterialia, 2011. **7**(5): p. 1999-2006.
7. Park, S.A., S.H. Lee, and W.D. Kim, *Fabrication of porous polycaprolactone/hydroxyapatite (PCL/HA) blend scaffolds using a 3D plotting system for bone tissue engineering.* Bioprocess and Biosystems Engineering, 2011. **34**(4): p. 505-513.
8. Ang, K.C., et al., *Investigation of the mechanical properties and porosity relationships in fused deposition modelling-fabricated porous structures.* Rapid Prototyping Journal, 2006. **12**(2): p. 100-105.
9. Lee, K.-w., et al., *Fabrication and Characterization of Poly(Propylene Fumarate) Scaffolds with Controlled Pore Structures Using 3-Dimensional Printing and Injection Moulding.* Tissue Engineering, 2006. **12**.
10. Khalyfa, A., et al., *Development of a new calcium phosphate powder-binder system for the 3D printing of patient specific implants.* Journal of Materials Science - Materials in Medicine, 2007. **18**(5): p. 909-916.
11. Fielding, G.A., A. Bandyopadhyay, and S. Bose, *Effects of silica and zinc oxide doping on mechanical and biological properties of 3D printed tricalcium phosphate tissue engineering scaffolds.* Dental Materials, 2012. **28**(2): p. 113-22.
12. Ge, Z., et al., *Proliferation and differentiation of human osteoblasts within 3D printed poly-lactic-co-glycolic acid scaffolds.* Journal of Biomaterials Applications, 2009. **23**(6): p. 533-547.

13. Gaetani, R., et al., *Cardiac tissue engineering using tissue printing technology and human cardiac progenitor cells.* Biomaterials, 2012. **33**(6): p. 1782-90.
14. Cohen, D.L., et al., *Direct freeform fabrication of seeded hydrogels in arbitrary geometries.* Tissue Engineering, 2006. **12**(5): p. 1325-1335.
15. Khalil, S. and W. Sun, *Bioprinting endothelial cells with alginate for 3D tissue constructs.* Journal of Biomechanical Engineering, 2009. **131**: p. doi: 10.1115/1.3128729.
16. Lee, C.H., et al., *Regeneration of the articular surface of the rabbit synovial joint by cell homing: a proof of concept study.* Lancet, 2010. **376**(9739): p. 440-448.
17. Skardal, A., et al., *Photocrosslinkable hyaluronan-gelatin hydrogels.* Tissue Engineering Part A, 2010. **16**(8): p. 2675-2685.
18. Skardal, A., J. Zhang, and G.D. Prestwich, *Bioprinting vessel-like constructs using hyaluronan hydrogels crosslinked with tetrahedral polyethylene glycol tetracrylates.* Biomaterials, 2010. **31**: p. 6173-81.
19. Censi, R., et al., *A printable photopolymerizable thermosensitive p(HPMAm-lactate)-PEG hydrogel for tissue engineering.* Advanced Functional Materials, 2011. **21**(10): p. 1833-1842.
20. Barry, R.A., et al., *Direct-write assembly of 3D hydrogel scaffolds for guided cell growth.* Advanced Materials, 2009. **21**(23): p. 2407-2410.
21. Engler, A.J., et al., *Matrix elasticity directs stem cell lineage specification.* Cell, 2006. **126**(4): p. 677-689.
22. Dhillon, A., et al., *Physical and biological characterisation of a novel injectable scaffold formulation.* Journal of Pharmacy and Pharmacology, 2010. **62**(10): p. 1510-1511.
23. Dhillon, A., et al., *Analysis of sintered polymer scaffolds using concomitant synchrotron computed tomography and in situ mechanical testing.* Journal of Materials Science - Materials in Medicine, 2011. **22**(12): p. 2599-2605.
24. Hamilton, L.G., R.A. Quirk, and K.M. Shakesheff, *An injectable scaffold for cell and growth factor delivery.* Journal of Pharmacy and Pharmacology, 2010. **62**(10): p. 1498-1499.
25. Rahman, C.V., et al., *Injectable scaffold for bone tissue engineering applications.* Journal of Pharmacy and Pharmacology, 2010. **62**(10): p. 1508-1509.
26. Boussahel, A., et al., *An injectable scaffold with sustained release of rhBMP2 for bone regeneration.* Journal of Pharmacy and Pharmacology, 2010. **62**(10): p. 1499-1500.
27. Rahman, C.V., et al., *Controlled release of BMP-2 from a sintered polymer scaffold enhances bone repair in a mouse calvarial defect model.* Journal of Tissue Engineering and Regenerative Medicine, 2012.
28. Morgan, E.F. and T.M. Keaveny, *Dependence of yield strain of human trabecular bone on anatomic site.* Journal of Biomechanics, 2001. **34**(5): p. 569-577.
29. Kopperdahl, D.L. and T.M. Keaveny, *Yield strain behavior of trabecular bone.* Journal of Biomechanics, 1998. **31**(7): p. 601-608.
30. Lotz, J.C., T.N. Gerhart, and W.C. Hayes, *Mechanical properties of trabecular bone from the proximal femur - a quantitative CT study.* Journal of Computer Assisted Tomography, 1990. **14**(1): p. 107-114.
31. Carter, D.R. and W.C. Hayes, *Bone compressive strength - influence of density and strain rate.* Science, 1976. **194**(4270): p. 1174-1176.
32. Malone, E. and H. Lipson, *Fab@Home: the personal desktop fabricator kit.* Rapid Prototyping Journal, 2007. **13**: p. 245-255.
33. Kirby, G.T.S., et al., *PLGA-based microparticles for the sustained release of BMP-2.* Polymers, 2011. **3**(1): p. 571-586.
34. Okamoto, T., et al., *Clonal heterogeneity in differentiation potential of immortalized human mesenchymal stem cells.* Biochemical and Biophysical Research Communications, 2002. **295**(2): p. 354-361.
35. Cohen, D.L., et al., *Additive manufacturing for in situ repair of osteochondral defects.* Biofabrication, 2010. **2**(3).
36. Goldstein, S.A., *THE MECHANICAL-PROPERTIES OF TRABECULAR BONE - DEPENDENCE ON ANATOMIC LOCATION AND FUNCTION.* Journal of Biomechanics, 1987. **20**(11-12): p. 1055-1061.
37. Goulet, R.W., et al., *THE RELATIONSHIP BETWEEN THE STRUCTURAL AND ORTHOGONAL COMPRESSIVE PROPERTIES OF TRABECULAR BONE.* Journal of Biomechanics, 1994. **27**(4): p. 375-389.
38. Tsuruga, E., et al., *Pore size of porous hydroxyapatite as the cell-substratum controls BMP-induced osteogenesis.* Journal of Biochemistry, 1997. **121**(2): p. 317-324.

39. Klawitter, J.J. and S.F. Hulbert, *Application of porous ceramics for the attachment of load bearing internal orthopedic applications.* Journal of Biomedical Materials Research Biomedical Materials Symposium, 1972. **2**: p. 161-229.
40. Robinson, B.P., et al., *Calvarial bone repair with porous D,L-polylactide.* Otolaryngology - Head and Neck Surgery, 1995. **112**(6): p. 707-13.
41. Whang, K., et al., *Engineering bone regeneration with bioabsorbable scaffolds with novel microarchitecture.* Tissue Engineering, 1999. **5**(1): p. 35-51.
42. Dormer, N.H., et al., *Osteochondral interface tissue engineering using macroscopic gradients of bioactive signals.* Annals of Biomedical Engineering, 2010. **38**: p. 2167-82.
43. Spalazzi, J.P., et al., *Development of controlled matrix heterogeneity on a triphasic scaffold for orthopedic interface tissue engineering.* Tissue Engineering, 2006. **12**(12): p. 3497-3508.
44. Curran, J.M., et al., *The osteogenic response of mesenchymal stem cells to an injectable PLGA bone regeneration system.* Biomaterials, 2013. **34**(37): p. 9352-9364.
45. White, L.J., et al., *Accelerating protein release from microparticles for regenerative medicine applications.* Materials science & engineering. C, Materials for biological applications, 2013. **33**(5): p. 2578-83.
46. Lee, J. and K.Y. Lee, *Local and sustained vascular endothelial growth factor delivery for angiogenesis using an injectable system.* Pharmaceutical Research, 2009. **26**(7): p. 1739-1744.
47. Kempen, D.H.R., et al., *Retention of in vitro and in vivo BMP-2 bioactivities in sustained delivery vehicles for bone tissue engineering.* Biomaterials, 2008. **29**(22): p. 3245-3252.
48. Kempen, D.H.R., et al., *Effect of local sequential VEGF and BMP-2 delivery on ectopic and orthotopic bone regeneration.* Biomaterials, 2009. **30**(14): p. 2816-2825.
49. Wang, F., et al., *Sustained release of insulin-like growth factor-1 from poly(lactide-co-glycolide) microspheres improves osseointegration of dental implants in type 2 diabetic rats.* European Journal of Pharmacology, 2010. **640**: p. 226-32.
50. Groeneveld, E.H. and E.H. Burger, *Bone morphogenetic proteins in human bone regeneration.* European journal of endocrinology / European Federation of Endocrine Societies, 2000. **142**: p. 9-21.
51. Luu, H.H., et al., *Distinct roles of bone morphogenetic proteins in osteogenic differentiation of mesenchymal stem cells.* Journal of Orthopaedic Research, 2007. **25**(5): p. 665-677.
52. Cho, T.-J., L.C. Gerstenfeld, and T.a. Einhorn, *Differential temporal expression of members of the transforming growth factor beta superfamily during murine fracture healing.* Journal of bone and mineral research : the official journal of the American Society for Bone and Mineral Research, 2002. **17**: p. 513-20.
53. Cheng, H., et al., *Osteogenic activity of the fourteen types of human bone morphogenetic proteins (BMPs).* The Journal of bone and joint surgery. American volume, 2003. **85-A**: p. 1544-52.
54. Qutachi, O., K.M. Shakesheff, and L.D.K. Buttery, *Delivery of definable number of drug or growth factor loaded poly(dl-lactic acid-co-glycolic acid) microparticles within human embryonic stem cell derived aggregates.* Journal of controlled release : official journal of the Controlled Release Society, 2013. **168**(1): p. 18-27.

Supplementary

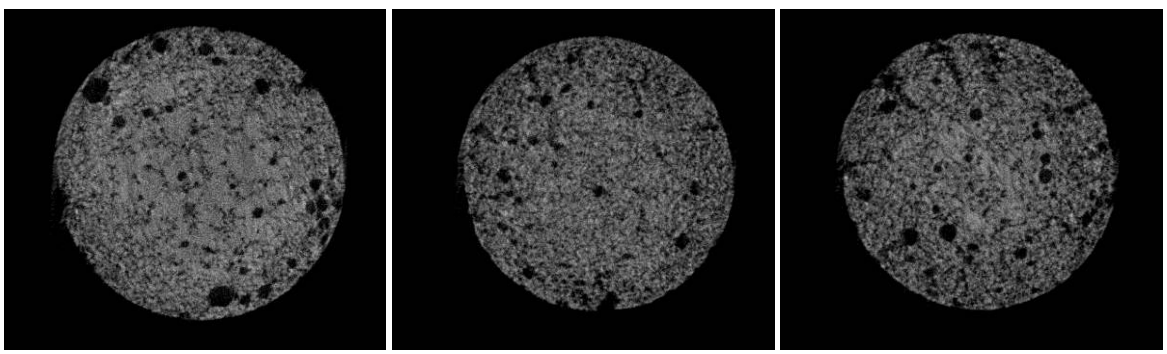

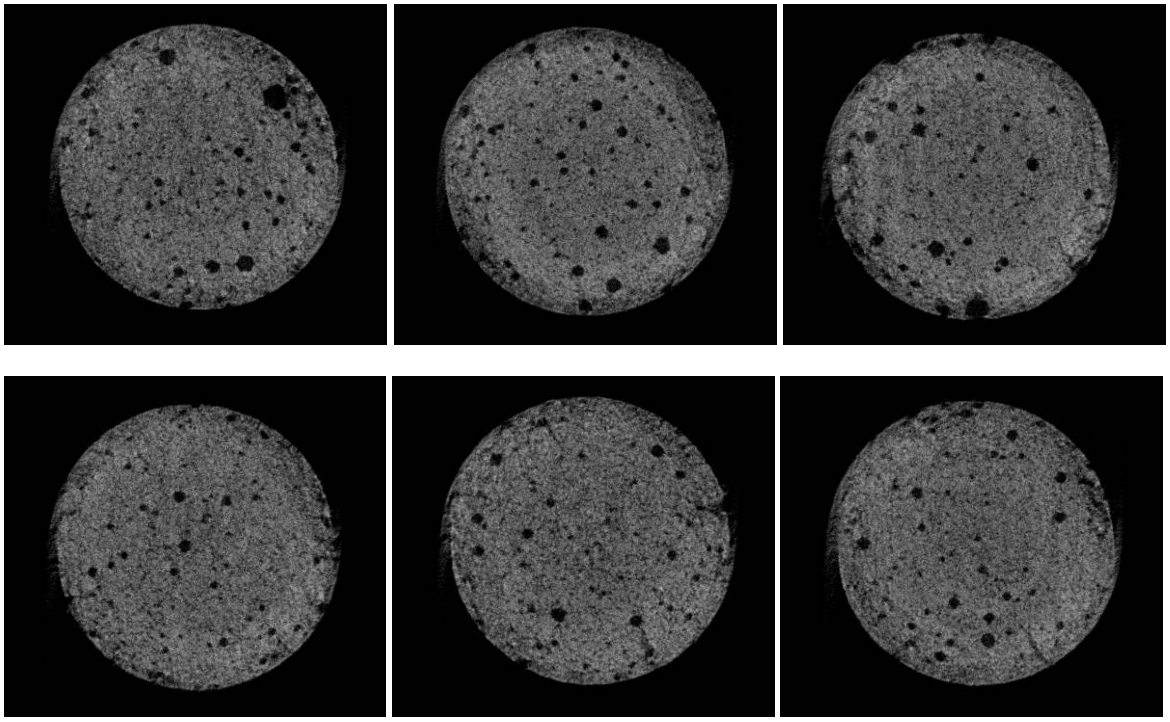

Figure 1. Micro-CT images were used to calculate porosity and pore size. From upper row to bottom row - 3% (w/v) medium viscosity CMC used at 1.4:1 (v:w) carrier to solid ratio, 2% (w/v) high viscosity CMC at 1.4:1 ratio and 3% (w/v) high viscosity CMC at 1.3:1 ratio.

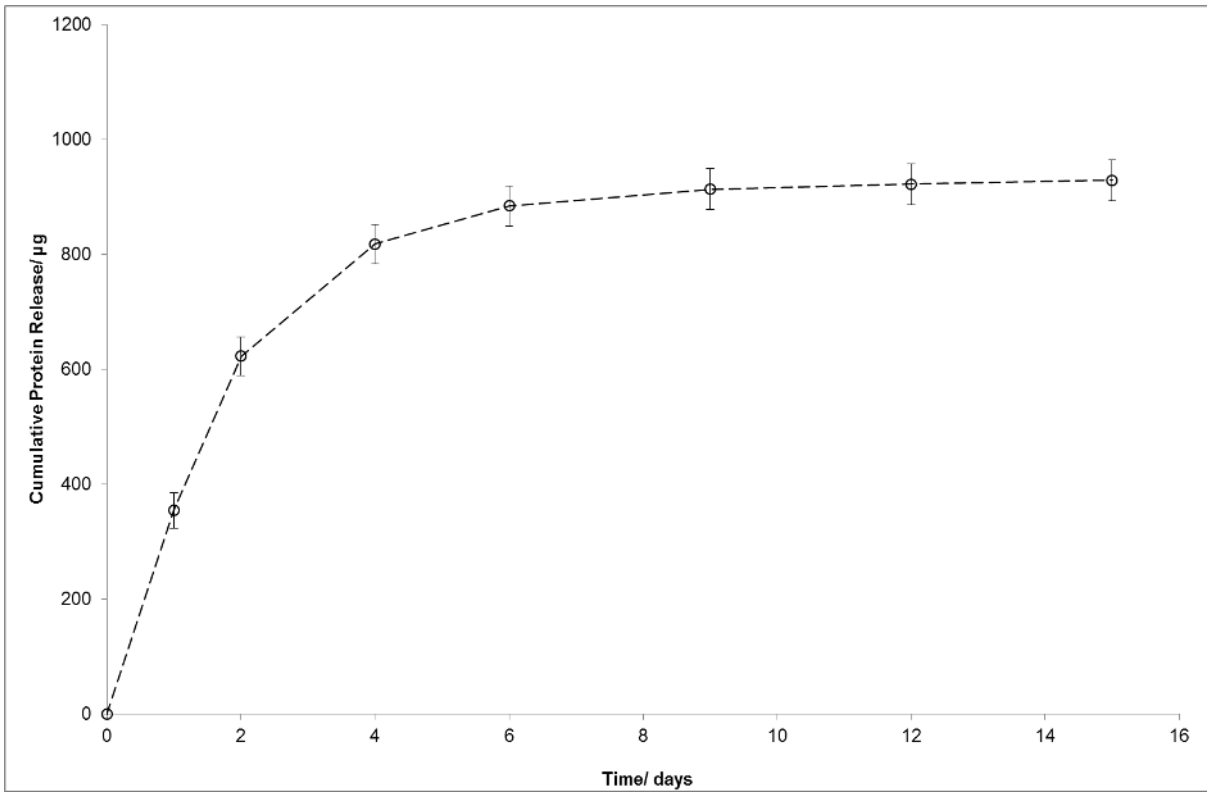

Figure 2. Lysozyme release from PLGA microspheres encapsulated within bioprinted PLGA-PEG microparticulate constructs (PLGA-PEG:PLGA=3:1 w/w). A 9:1 (w:w) mixture of HSA and lysozyme

was encapsulated in PLGA microspheres via a double emulsion protocol with a total protein content of 1% (w/w) relative to polymer.